Numerical simulation of drop formation in a T-shaped microchannel

J.L. Liow [1]

[1]Mechanical Engineering Discipline, School of Engineering
James Cook University, Qld, 4811 AUSTRALIA

Abstract

The formation of water drops of specific size when sheared by a tetradecane stream at a T-junction in a microchannel was investigated numerically. The numerical results showed that the water drop sizes decreased with increasing tetradecane flow rate and decreasing interfacial tension. This is in agreement with published experimental results. During the formation of the water drops, two recirculating zones are formed in the water stream, a large one occupying most of the water drop, and a smaller one near the downstream corner of the T-junction. The smaller recirculating zone results in a high pressure spot.

Introduction

In the last two decades, the emphasis on fluid flow in MEMS devices has been focused on the study of single fluid flows, involving only a gas or a liquid [4]. In contrast, the dispersion of the droplets of one fluid in a second immiscible fluid has received less attention. Nevertheless, there is a wide range of applications for multiphase flows in microchannels and such flows are found in naturally occurring systems. The ability to control and manipulate the drop size and frequency enables the drop formation process to be tailored. This is of immense importance as it allows the outcomes of the applications to be very specific. In recent years, the use of microchannels for the formation of drops of uniform and specific sizes has been shown experimentally to be feasible. However, there is a wide range of microchannel configurations that have been published and the drop formation processes are quite different for different configurations. The simplest configuration is the T-junction where one liquid shears a second liquid that flows in the perpendicular arm.

Early work by Thorsen *et al.* [13] showed that aliphatic straight chained hydrocarbons (HC) with 2% SPAN 80 were able to shear a normal flow of water to form a variety of drop shapes. The drop shapes were strongly dependent on the sharpness of the edges of the T-junction. Further work by Tabeling *et al.* [12] suggests that such drops can only be formed when the surface tension of the HC is significantly lowered by SPAN 80 used as the surfactant. The roughness of the channel surface also plays a critical role in the drop formation process. In contrast, Nisisako *et al.* [7] managed to form droplets without the use of surfactants albeit the channels they used were $100-500\ \mu$m in width and 100 μm in depth compared to 35 μm in width for the work of Thorsen *et al.* [13] and Tabeling *et al.* [12]. Apart from channel size, there were a few significant differences between Thorsen *et al.* [13] and Nisisako *et al.* [7]. First, Nisisako *et al.* [7] used a sunflower oil where the fluid properties were not measured but sunflower oil does have a much higher kinematic viscosity than straight chained HC. Second, Nisisako *et al.* [7] produced their microchannels with a micromilling technique resulting in extremely sharp corners. Thorsen *et al.* [13] produced their microchannels from moulding with an acrylated urethane where the corners are much smoother.

Other more complex configurations include the use of multiple slits to focus the flow and produce drops that are much smaller than the slit width [1], or the use of fine pores and stepped structures to try and produce reproducible drop sizes [11]. More complex network of T-junctions have been shown to enable drop size distributions to be controlled (Link *et al.* as referenced in [10]). The control of drop breakup is influenced significantly by the interfacial tension between the two fluids and Dreyfus *et al.* [3] have found that without the presence of Span80, drops do not form in microchannels of 20 μm by 200 μm cross section.

In this study, a T-junction microchannel is numerically simulated using a volume of fluid (VOF) code in 2D to determine the breakup of water drops entering into a flow of tetradecane. This is compared to the experimental result of Cole [2]. Although the depth of the channel may affect the drop formation, much information can be obtained of the behaviour of the drop break up characteristics in 2D prior to a full simulation in 3D.

Mathematical formulation

Detailed description of the multifluid VOF (MFVOF) code has been published elsewhere [5] and only a brief description will be included here.

The distribution of the fluid species is tracked as a "colour" C where in the continuous limit within a computational domain represented by a 2D axisymmetric mesh, $C(r,z)$ is the Heaviside function

$$C = \begin{cases} 1, & \text{if point } (r,z) \text{ is occupied by } C \text{ fluid;} \\ 0, & \text{otherwise.} \end{cases} \quad (1)$$

All interfaces throughout the computational domain are deduced from the spatial locations of the discontinuities in the distribution of C. The equations solved are:

Equation of continuity

$$\nabla \cdot \mathbf{U} = 0. \quad (2)$$

Fluid species transport equation

$$\frac{\partial C}{\partial t} + \nabla \cdot (\mathbf{U}C) = 0. \quad (3)$$

Momentum equation

$$\frac{\partial \mathbf{U}}{\partial t} + \nabla \cdot (\mathbf{UU}) = -\frac{1}{\rho}\nabla P + \frac{1}{\rho}\nabla \cdot \tau + g + \frac{\mathbf{S}}{\rho}, \quad (4)$$

where $\tau_{ij} = 2\mu S_{ij}$ and the rate of strain tensor, $S_{ij} = (\partial u_i/\partial x_j + \partial u_j/\partial x_i)/2$. The effects of surface tension are incorporated in the surface force vector

$$\mathbf{S} = S_r\hat{i} + S_t\hat{j} = \sigma\kappa\hat{n}, \quad (5)$$

which is applied only at interfaces. The interfacial curvature κ and interfacial normal $\hat{n}$ are functions of C. The density and viscosity distributions are dependent on the distribution of fluid throughout the flow domain, and are computed from C of the
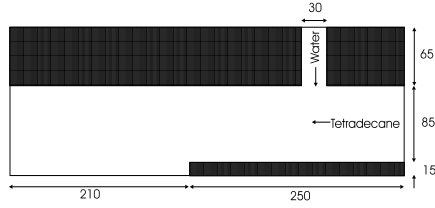
Figure 1: The simulation region. Dimensions are given in μm.

number of fluid species (nsp) using weighted averages of the form

$$\rho = \sum_{l=1}^{nsp-1} C_l \rho_l + \left(1 - \sum_{l=1}^{nsp-1} C_l\right) \rho_{nsp}. \qquad (6)$$

Discretisation and Solution Algorithm

The equations are discretised on a uniform MAC mesh using second-order accurate conservative finite differencing schemes. The time advance of the solution from timestep n to $n+1$ is achieved using a two-step projection method, which decomposes the algorithm for the flow solver into three core steps:

- estimate the solution at the next timestep by including all numerical schemes for modelling all physics in the problem,

- solve a Poisson equation, for which the source term is the divergence from a solenoidal velocity field,

- correct the momentum update velocity estimate, to update the velocity field to timestep $n+1$.

An explicit scheme is used in the MFVOF solution algorithm for the time advance. Second-order temporal accuracy is achieved using Euler time-stepping, which involves performing the two-step projection twice. The color function in the discretised problem is only an approximation of the Heaviside function, and on the mesh is interpreted as a fractional volume function. The value of C in interface cells is simply taken as the volume fraction of the mesh cell volume occupied by $C-$fluid.

Layout of the microchannel

The T-junction microchannel simulated is shown in Figure 1. Water flows downwards in the vertical channel of 30 μm and tetradecane flows in the horizontal channel of 85 μm from right to left. Away from the T-junction, the horizontal channel widens to 100 μm to allow the drops to disengage. The mesh used was a 64 and 192 cells in the vertical and horizontal directions respectively. The physical properties of the fluids are given in Table 1. No-slip boundary conditions were used and a flat inlet velocity profile was used for both liquids streams.

Results

Simulations were carried out for varying tetradecane velocities for two different water inlet velocities with no surfactant added. The water droplets formed were uniform in size and shown in Figure 2. It was found that a straight line relationship could be obtained for water drops less than 100 μm as a function of the tetradecane velocity. There was no difference in the diameter of the water drops for water flow velocities of 0.01 and 0.05 m/s. The relationship fitted is

$$d = -15.9 \ln V + 36.77, \qquad (7)$$

Water	
Density	998.2 kg/m^3
Viscosity	1.0×10^{-3} kg/(m·s)
Tetradecane	
Density	773.0 kg/m^3
Viscosity	3.19×10^{-3} kg/(m·s)
Interfacial tension	0.0442 N/m
Temperature	20°C

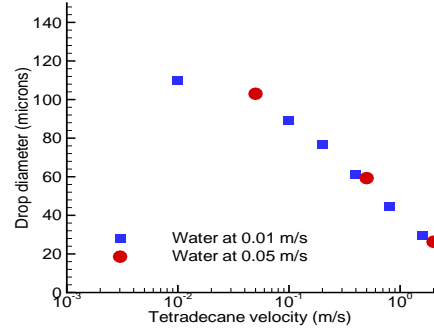Table 1: Properties of the fluids used in the simulation.

Figure 2: Water drop size as a function of tetradecane flow velocity.

where d is the water drop diameter in microns and V is the tetradecane velocity in m/s. A previous numerical simulation of a similar T-junction by Reedman [8] for a T-junction where both channels were 30 μm in size is shown in Figure 3. It can be seen that a linear relationship exists for water drops formed that are smaller than 50 μ in diameter. However, as the water flow velocity is increased, the water drops formed increase in size for the same tetradecane flow rate so that there is a different linear relationship for each water flow velocity. The main difference between the current results and [8] is that in Reedman's results, the water drops formed are all larger than the channel width, while in the current work most of the drop sizes are smaller than the channel width. The experimental results of Nisisako *et al.* [7] and that of Liow and Cole [6] are shown in Figure 4. For water drops that are smaller or close to the oil/HC channel width, there is a straight line relationship. In Nisisako's case, the oil inlet channel is 500 μm, and the water drops formed are all smaller than the oil channel and do not give rise to slug flow. For Liow and Cole, the lower tetradecane flow rates re-
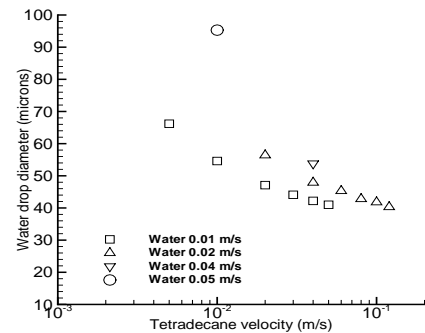

Figure 3: Results of Reedman [8] for water drop size as a function of tetradecane flow velocity for a 30 μm width channel.
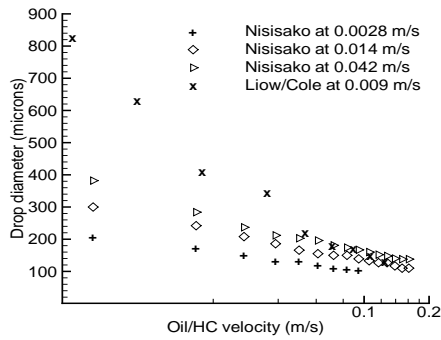
Figure 4: The experimental results of Nisisako [7] and Liow and Cole [6]. For Nisisako, the channel widths are 100 μm for the water and 500 μm for the oil. For Liow and Cole, the channel widths are both 250 μm.
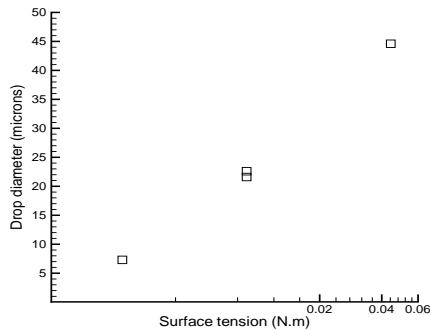

Figure 5: Effect of interfacial tension on the water drop size formed. The two data points for a interfacial tension of 0.0089 N·m were carried out at mesh resolution of 64 × 192 and 128 × 384.

sult in large drops that slugs down the channel. Consequently, drops larger than 250 μm do not follow the straight line fit for the smaller drops.

Effect of reducing interfacial tension

Experimentally [6, 10, 13] it has been shown that when surfactants are not used for the formation of water drops in small channels, the water and oil/HC streams form separate parallel flow channels. The reduction in interfacial tension was simulated for a case where the water and tetradecane flow velocities were 0.01 and 0.8 m/s respectively. Figure 5 shows the dramatic effect the drop size decreasing with a reduction in the interfacial tension. As the interfacial tension is reduced to 0.0089 N/m, satellite drops are formed. A high order resolution of the mesh used (128 × 1024) to check the results showed that satellite drops were not a result of the lower mesh resolution. Moreover, the large water drops formed differed only by 4% in diameter (1μm) between the two mesh resolutions, which was of the order of 1 mesh size. This effect was not seen experimentally by [6] but the water/tetradecane flow ratios in the simulation are much higher. However, satellite drops have been found in the flow focussing experiments of Anna *et al.* [1]. For the control of drop sizes, the presence of the satellite drops as the interfacial tension is reduced means that smaller drops are always present. The presence of the satellite drops are not desired if the aim is to produce a fixed particle size. Figure 6 shows the drop formed for the three different surface tension cases. As the interfacial
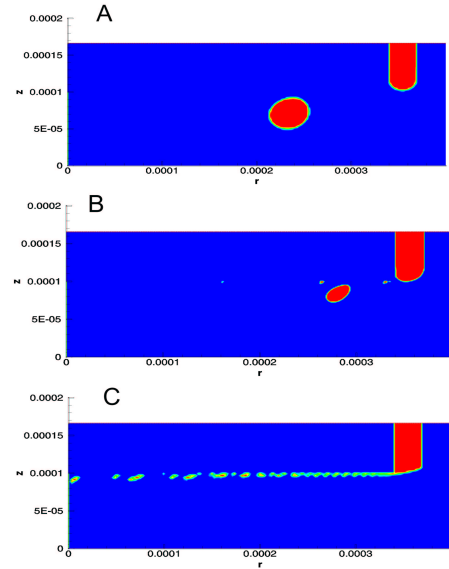

Figure 6: Drop formation for varying surface tension A: 0.0442 B: 0.0089 C: 0.0022 N/m. Water 0.01 m/s, Tetradecane 0.8 m/s.

tension is reduced, the drop is stretched much more in the flow. Interestingly, the satellite drops that are formed remain close to the channel boundary and hence move with a much lower velocity. This may provide a means of separating the larger and smaller drops if satellite drop formation is unavoidable.

Drop generation

Figure 7 shows the velocity vectors and associated pressure contours at the T-junction for the first four milliseconds from the numerical simulation. The drop detaches just after 4 ms. The velocity profile of the tetradecane stream is parabolic, the profile being established within a few μm from the inlet. The pressure gradient along the tetradecane channel decreases linearly with distance. In the first ms, the pressure in the water stream initially increases throughout the channel to overcome the interfacial forces to form a hemispherical cap. The velocity of the tetradecane stream creates a velocity gradient in the hemispherical cap resulting in a localised recirculating flow. The tetradecane stream also distorts the interface slightly resulting in an asymmetric pressure distribution around the hemispherical cap.

At 2 ms, the drop has protruded far enough that the tetradecane stream shears it in the downstream direction. The recirculating flow in the water section has grown in magnitude and is concentrated in the section that protrudes into the tetradecane section. The tetradecane approaching the water protrusion is forced to accelerate as the cross sectional area for flow is reduced. Far downstream, the tetradecane flow regains its parabolic flow profile. The velocity vectors show a smaller co-rotating recirculating flow at the downstream corner of the T-junction. The centres of the two recirculating zones show up in the pressure contours as a high pressure spot, with the smaller co-rotating recirculating zone having a higher peak pressure. The presence of the two recirculating zones that are in the same direction suggests that the flow set up by the tetradecane splits into two stream, the larger one moving into the drop that is being formed, while the smaller one moves towards the downstream corner.

At 3 ms and 4 ms, the smaller co-rotating recirculating zone continues to grow in size while the larger co-rotating zone moves out further into with the water drop. The pressure in the larger co-rotating zone smears out to a more uniform value,
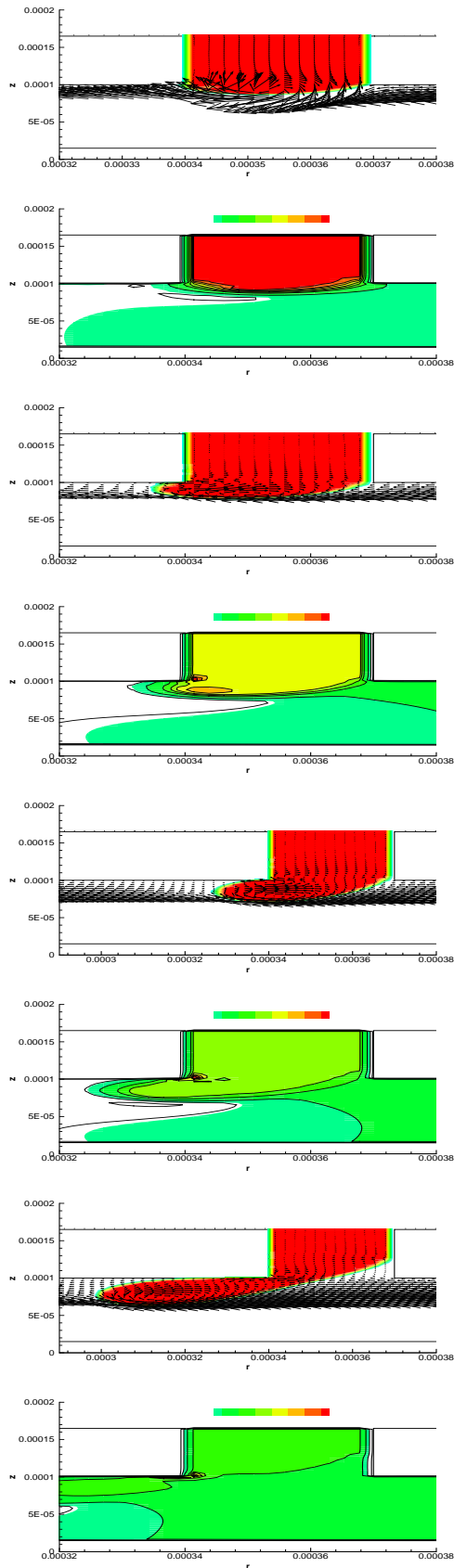
Figure 7: Velocity vectors and corresponding pressure contours at the T-junction for successive time intervals of 1, 2, 3 and 4 ms respectively from top to bottom. Water 0.01 m/s, Tetradecane 1.6 m/s.

as the drop grows rapidly since the interfacial forces holding the larger drop shape decreases when the drop is past a hemispherical shape. Throughout the growth of the water drop, the pressure at the downstream corner is still the highest. This has implications for drop formation in that the sharp corner significantly affects the pressure and flow characteristics in the formation of the water drop. The use of a rounded corner would be expected to reduce the pressure buildup there.

Conclusions

This study of water drops forming into a stream of tetradecane at a microchanneled T-junction has shown that the water drop size decreases with increasing tetradecane velocity and decreasing interfacial tension. The numerical results are in line with published experimental results. It was found that a high pressure recirculating zone builds up at the downstream corner of the T-junction and the use of a rounded corner for controlling the drop formation process should be investigated in the future.

References

[1] Anna S. L., Bontoux N., and Stone H. A., Formation of dispersions using "flow focusing" in microchannels. *Applied Physics Letters*, **82(2)**, 2003, 364–366.

[2] Cole D. *Microdevice Construction and Application for Multiphase Microflows*. Final year thesis, James Cook University. 2003.

[3] Dreyfus R., Tabeling P., and Willaime H., Ordered and disordered patterns in two-phase flows in microchannels. *Phys. Rev. Lett.*, **90**, 2003, 144505.

[4] Gad-el-Hak M., The fluid mechanics of microdevices The Freeman Scholar lecture. *J. Fluids Engng.*, **121**, 1999, 5–33.

[5] Liovic P., Rudman M. and Liow J. L. Numerical modelling of free surface flows in metallurgical vessels. *Appl. Maths. Modelling*, **26**, 2002, 113–140.

[6] Liow J. L., and Cole D. Drop formation in T-junction microchannels. in *Chemeca conference 2004*, Sydney, Australia, 2004, 6pp.

[7] Nisisako T., Torii T. and Higuchi T., Droplet formation in a microchannel network. *Lab on a Chip*, **2**, 2002, 24–26.

[8] Reedman, M. *Numerical simulation of microflows.* Final year thesis, James Cook University. 2002.

[9] Stone, H. A. and Kim, S., Microfluidics: Basic issues, applications, and challenges. *AIChE Journal*, **47(6)**, 2001, 1250–1255.

[10] Stone H. A., Stroock A. D. and Ajdari A., Engineering flows in small devices: Microfluidics toward a lab-on-a-chip. *Annu. Rev. Fluid Mech.*, **36**, 2004, 381–411.

[11] Sugiura S., Nakajima M., and Seki M., Interfacial tension driven mondispersed droplet formation from microfabricated channel array. *Langmuir*, **17**, 2001, 5562–5566.

[12] Tabeling M., Some basic problems of microfluidics in *14th Australasian Fluid Mechanics Conference*, Adelaide University, Adelaide, Australia, 2001, 57–62.

[13] Thorsen T., Roberts R. W., Arnold F. H. and Quake S. R., Dynamic pattern formation in a vesicle-generating microfluidic device. *Phys. Rev. Letters,* **86**, 2001, 4163–4166.